PERFORMANCE EVALUATION OF SEVERAL HIGH-QUALITY DIGITAL CAMERAS

D. H. Rieke-Zapp [a], W. Tecklenburg [b], J. Peipe [c], H. Hastedt [d], T. Luhmann [b]

[a] Institute of Geological Sciences, University of Bern, Baltzerstrasse 1+3, 3012 Bern, -Switzerland – zapp@geo.unibe.ch
[b] Institute of Applied Photogrammetry and Geoinformatics, University of Applied Sciences Oldenburg/Ostfriesland/Wilhelmshaven, Ofener Strasse 16/19, 26121 Oldenburg, Germany – (werner.tecklenburg@fh-oow.de – thomas.luhmann@fh-oow.de)
[c] University of the Federal Armed Forces, 85577 Neubiberg, Germany – j-k.peipe@unibw-muenchen.de
[d] Swiss Federal Research Institute for Forest, Snow and Landscape Research, Zuercherstrasse 111, 8903 Birmensdorf, Switzerland - heidi.hastedt@wsl.ch

Commission V, WG V/1

KEY WORDS: Geometric stability, camera calibration, accuracy assessment, digital camera

ABSTRACT:

The accuracy of object reconstruction was tested for six high quality digital cameras. Nikon D80, D200, D2X and D3 with the same 24 mm Nikon lens, a Canon EOS 5D with a normal as well as a stabilized 35 mm Canon lens and an Alpa 12 WA with special fixation of a digital camera back and lens were evaluated. All cameras were investigated on a test cube that was designed according to VDI/VDE 2634, a German standard for evaluation of optical 3-D measuring systems. The measuring volume was approximately 2000 mm x 2000 mm x 1600 mm (length x width x height). Seven scale bars with up to ten calibrated distances on them were placed in the cube to evaluate the length measurement error (LME). Images were imported into a PC and analyzed with AICON 3D Studio software. Calibration was performed with a standard set of parameters as well as with an image variant set of parameters to account for geometric instabilities and to reveal the potential accuracy of the cameras. The smallest LME for calibration with standard parameters was achieved with 0.047 mm using the Canon EOS 5D and a stabilized 35 mm lens. For calibration with image variant parameters the Alpa 12 WA performed best with a maximum absolute LME of 0.029 mm. Geometric accuracy was significantly reduced in cases where a ringflash was screwed into the filter thread of the lens. Only the Canon EOS 5D with stabilized lens was unaffected by the extra load of the ringflash. Subsequent evaluation of the Nikon D2X and D3 with ringflash mounted to the cameras' tripod mount revealed similar LME of 0.052 and 0.059 mm, respectively, as for the Canon camera when calibrating with the standard set of parameters. The other Nikon cameras and the Alpa camera were only evaluated with the ringflash mounted to the lens.

1. INTRODUCTION

High quality digital cameras provide standard tools for photogrammetric surveys for several years now (Peipe and Schneider, 1995). Although they were not designed for photogrammetric applications, the accuracy that can be accomplished with regular cameras is remarkable, but often limited by the geometric stability of the cameras (Gruen et al., 1995; Maas, 1999; Shortis et al., 2006). Different investigations have been made to model or compensate for the instable geometry of non-photogrammetric cameras.

Conventional mathematical models for camera calibration assume a constant interior orientation for one set of images over the whole period of image acquisition. Principal distance (c), principal point (x'_0, y'_0), radial-symmetric lens distortion (A_1, A_2, A_3), decentring of lenses by tangential and asymmetric distortion (B_1, B_2) and global sensor properties such as affinity and shear (C_1, C_2) are estimated within self-calibrating systems. It can not be assumed that camera parameters remain stable over the whole period of image acquisition. As examples, extended mathematical models include parameterization of image variant interior orientation (Maas, 1999; Tecklenburg et al., 2001), the calculation of additional parameters for modeling the influence of sensor distortion (Tecklenburg et al., 2001) or gravitational effects (Haig et al., 2006).

Alternatively mechanical stabilization can be used to compensate for instabilities, e.g. by fixing the sensor inside the camera (Shortis et al., 2001; Rieke-Zapp & Nearing, 2005) or fixation of optical lenses, as it is presented within these investigations. In addition the usage of other hardware components is investigated, e.g. a ringflash that is not mounted to the filter thread of the lens in order to unload the weight of the ringflash off the lens.

Whereas a mechanical stabilization will typically void the manufacturer's warranty and the flexibility in the usage of components, the parameterization of camera instabilities using an image variant setup is not accepted as a standard parameter set in practice. Only some software products like AICON 3D Studio (AICON, 2007) or AXIOS 3D AX.Ori (AXIOS, 2008) support image-variant calculations.

Six cameras were evaluated in order to test the accuracy that can be accomplished with different camera setups and to identify reasons for geometric instability as well. The investigations include both mechanical stabilization and parameterization models. All cameras were investigated on a

test cube that was designed according to VDI/VDE 2634, a German standard for evaluation of optical 3-D measurement systems (VDI/VDE, 2002).

In this paper we use ΔL for length measurement error of one given distance in the test cube to separate these values strictly from the maximum absolute length measurement error denoted as LME.

2. MATERIALS AND METHODS

2.1 Evaluated Cameras

Six different cameras of three different manufacturers were evaluated (Table 1). All cameras were used with a ringflash screwed into the filter thread of the lens. Additionally the Nikon D2X and D3 were also tested with the ringflash mounted to the cameras' tripod mount. The Canon EOS 5D was evaluated with a standard EF 2/35 mm lens as well as with a similar lens where the inner lens tube was fixed with epoxy (Figure 1).

Camera	Alpa 12 WA	Canon EOS 5D	Nikon		
			D3	D2X	D80 D200
Focal length (mm)	47	35	24	24	24
Diagonal field of view	65°	63°	84°	61°	61°
Sensor (mm^2)	36x48	24x36		16x24	
Pixel (y)	4992	2912	2832	2848	2592
Pixel (x)	6666	4368	4256	4288	3872
Pixel size (μm)	7.2	8.2	8.5	5.5	6.1
Stabilization method	back & lens	lens epoxy	-/-	-/-	-/-

Table 1. Specifications of evaluated cameras.

Figure 1. Canon EOS 5D with EF 2/35 mm lens where the focusing tube was fixed with epoxy (indicated by the whitish ring around the focusing tube).

In case of the Alpa 12 WA the digital back, a Leaf Aptus 75, and the lens were fixed with screws to the camera body (Figure 2). The focal lengths of the lenses were chosen to provide a similar field of view for all cameras, but for the Nikon D3 (Table 1). The same AiS Nikkor 2.8/24 mm Nikon lens was used on all Nikon cameras to exclude the effect of different lenses to the results for this group. The digital sensor of the D3 is much larger than for the other Nikon models resulting in a wider angle of view and therefore a slightly different perspective than for the other cameras. The sensor sizes of the cameras range between 16 x 24 and 36 x 48 mm^2 meaning that the sensor inside the Leaf Aptus 75 digital camera back is more than four times as large as the sensor of the Nikon D2X. The Nikon D2X has the smallest pixel size of all cameras (Table 1). All images were recorded as raw data and converted to TIFF for analysis in the software supplied with the digital camera device. While Nikon and Canon cameras are digital single lens reflex cameras, the Alpa has no mirror in the optical path. An external viewfinder is used to frame the images with the Alpa (Figure 2).

Figure 2. Alpa 12 WA with digital back and lens fixed with screws to the camera body.

2.2 Calibration procedure

The different camera setups were investigated on a test cube (Figure 3) that was designed according to VDI/VDE 2634 (VDI/VDE, 2002). The measuring volume was approximately 2000 mm x 2000 mm x 1600 mm (length x width x height). Seven scale bars with up to ten calibrated distances on them were placed in the cube to evaluate the maximum absolute length measurement error (LME). In total, 58 calibrated distances were available, all calibrated to an accuracy of 0.010 mm and better. 185 retro-reflective targets were attached to the cube. A single system scale was placed in the centre of the cube. Images were acquired in the same configuration for each camera setup. Approximately 120 images were taken from 12 positions around the cube at three different heights (Figure 4). All images were taken with a ringflash mounted to the camera or the filter thread of the lens. Several images of each setup were taken with the camera rotated about the principal axis to minimize correlation of parameters of interior orientation. Images were imported into a PC and analyzed with AICON 3D Studio software (version 7.5; AICON, 2007). Two calibrations were calculated for each setup. In the first calibration, here denoted as standard procedure, the interior orientation of the cameras with the position of the projection centre in image

space (c, x'_0, y'_0) was calibrated along with additional parameters for lens distortion (A_1, A_2, A_3, B_1, B_2) as well as affinity and shear (C_1, C_2). In a second setup the same parameters were used for calibration, but the parameters of interior orientation were calculated separately for each image thus accounting for geometric instability of the principal point and/or the camera constant (Tecklenburg et al., 2001; Hastedt et al., 2002; Rieke-Zapp et al., 2005).

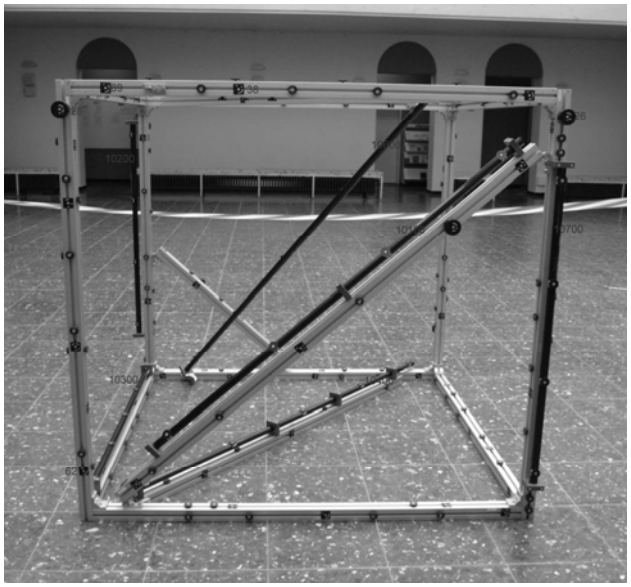

Figure 3. Testfield according to VDI/VDE 2634 with seven measuring lines and retro-reflective target points.

Figure 4. Bundle design containing 120 images, top and front view.

3. RESULTS AND DISCUSSION

3.1 Standard calibration

Results of calibration with the standard parameter set and without parameterization of geometric instabilities showed good results only for the three setups where the ringflash was either not mounted to the lens (Nikon D2X, D3; Figure 5) or the lens tube was fixed with epoxy (EOS 5D) (Figure 1, Table 2). Loading the filter thread of the lenses with the weight of the ringflash had strong negative effects on the accomplished accuracy. Working with a ringflash in the filter thread of the lens was considered as a common practice for close range photogrammetric applications (Haig et al., 2006). Fixing the lens tube of the EOS 5D setup has improved the -LME from 0.330 to 0.047 mm – an improvement by a factor of seven (Table 2).

Figure 5. Mounting of the ringflash to the cameras' tripod mount to relieve the filter thread of the lens off the extra load.

Camera	LME (mm)
Alpa 12 WA	0.124
Canon EOS 5D – standard lens	0.330
Canon EOS 5D – fixed lens tube	0.047
Nikon D80	0.191
Nikon D200	0.208
Nikon D2X – ringflash fixed to lens	0.166
Nikon D2X – ringflash fixed to camera†	0.059
Nikon D3 – ringflash fixed to lens	0.213
Nikon D3 – ringflash fixed to camera	0.052

† only JPEG images available

Table 2. Maximum absolute length measurement error (LME) for standard calibration with AICON 3D Studio.

Camera	ΔL min. (mm)	ΔLmax. (mm)
Canon EOS 5D – standard lens	-0.330	+0.303
Canon EOS 5D – fixed lens tube	-0.047	+0.047
Nikon D3 – ringflash fixed to lens	-0.129	0.213
Nikon D3 – ringflash fixed to camera	-0.041	+0.052

Table 3. Interval of length measurement error ΔL for standard calibration with AICON 3D Studio.

In case of the Nikon cameras unloading the lens off the ringflash improves the LME by a factor of 3 to 4 (Figure 5). As the lens tube was not fixed in the Nikon 24 mm lens, slight

movements of the lens tube caused by gravity were still possible even without the ringflash in place. Figure 6 shows a comparison for the Nikon D2X ΔL results where the standard calibration method with the externally mounted ringflash is plotted versus an image variant parameterization for ringflash mounted to the lens. It illustrates the improvement in object accuracy with a standard parameterization using simple mechanical components, besides the improvement in accuracy compared to the standard calibration with the lens mounted ringflash.

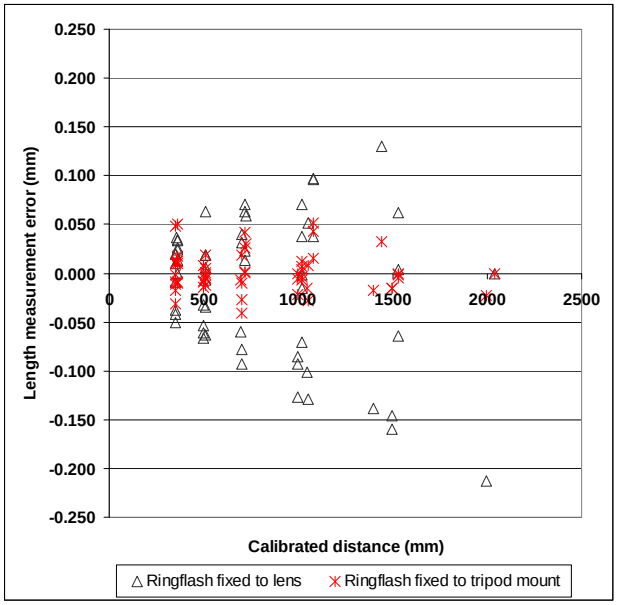

Figure 5. Length measurement errors ΔL of the Nikon D3 with ringflash fixed to the lens and fixed to the tripod mount of the camera.

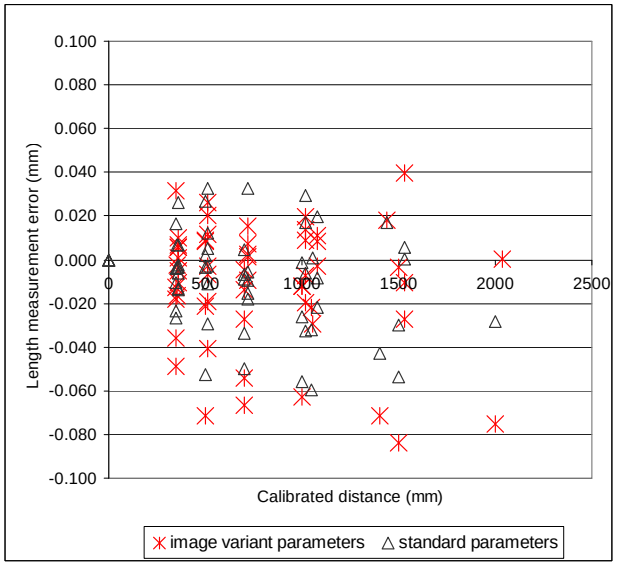

Figure 6. Length measurement errors ΔL of the Nikon D2Xwith ringflash fixed to the lens and image variant parameterization versus ringflash fixed to the tripod mount of the camera and standard parameterization.

Results of the other cameras were probably also strongly affected by loading the lenses with the ringflash.

A comparison of different Nikon models from consumer (D80) over semi-professional (D200) to professional (D2X, D3) models was only possible for calibrations with the ringflash mounted to the lens. For this setup no significant difference was visible for the different camera models (Table 2). Any existing difference in camera stability was probably hidden by the adverse effects of the ringflash.

3.2 Calibration with image variant interior orientation

Calculation of calibration parameters with image variant interior orientation compensated for geometric instability of the principal point and/or the camera constant (Tecklenburg et al., 2001). For all cameras, but the EOS 5D with the lens where the focusing tube was fixed with epoxy, results improved significantly from the standard calibration (Tables 3 and 4). The best LME resulted to 0.029 mm and was accomplished with the Alpa 12 WA camera. In case of the EOS 5D, parameterization of geometric instabilities by an image variant interior orientation yielded almost the same results as fixing the lens tube with epoxy and working with the standard set of parameters (Tables 2, 3). For the Nikon camera series only the Nikon D3 showed a significant gain in accuracy compared to the other cameras. The resulting LME for the Nikon D3 slightly improved when fixing the ringflash not to the lens, indicating that the calibration with the image variant interior orientation did not completely compensate for the adverse effects of the ringflash.

It was not clear why the maximum absolute LME for the EOS 5D with epoxy fixing of the lens was deteriorated when image variant interior orientation was applied (Figure 7). For the standard calibration all ΔL ranged between +0.047 and -0.047 mm while for the image variant calibration the values ranged between -0.066 and +0.038 mm (Figure 7, Table 5). The ΔL results for standard calibration were well distributed around zero from maximum to minimum without any gross outliers. Checking the results for the image variant calibration revealed a larger amplitude of ΔL. A similar effect was visible for the calibration of the same camera without fixation of the lens tube. For standard calibration the ΔL ranged between +0.330 and -0.303 mm, but showed much more skew for the image variant calibration with ΔL ranging between +0.047 and -0.022 mm. Although the LME improved significantly in the latter case, the ΔL revealed larger skew. A similar trend was also visible for other cameras where the LME improved significantly with image variant calibration. Although most ΔL values were smaller than for the standard calibration, the extreme values became larger with the extreme drifting stronger in positive or negative direction. Generally the ΔL was not correlated with the distance of the measuring line. The largest absolute deviations were in most cases observed for shorter distances up to 700 mm (Figures 5, 7, 8). Minimum and maximum ΔL for the Alpa and the Nikon D3 with image variant calibration had almost the same absolute value. ΔL values ranged between +0.029 and -0.028 mm for the Alpa, and between +0.046 and -0.035 mm and +0.039 and -0.028 mm for the Nikon D3 with and without ringflash mounted to the lens, respectively (Table 5).

Camera	LME (mm)
Alpa 12 WA	0.029
Canon EOS 5D – standard lens	0.046
Canon EOS 5D – fixed lens tube	0.066
Nikon D80	0.093
Nikon D200	0.081
Nikon D2X – ringflash fixed to lens	0.083
Nikon D2X – ringflash fixed to camera	-/-
Nikon D3 – ringflash fixed to lens	0.046
Nikon D3 – ringflash fixed to camera	0.039

Table 4. Maximum absolute length measurement error LME for calibration with image variant interior orientation using AICON 3D Studio software.

Camera	ΔL Min (mm)	ΔL max (mm)
Alpa 12 WA	-0.028	+0.029
Canon EOS 5D – standard lens	-0.022	+0.047
Canon EOS 5D – fixed lens tube	-0.066	+0.038
Nikon D3 – ringflash fixed to lens	-0 .025	+0.046
Nikon D3 – ringflash fixed to camera	-0.028	+0.039

Table 5: Interval of length measurement error ΔL for image variant interior orientation using AICON 3D Studio software.

If the distribution of ΔL is plotted against the calibrated distances of the measuring lines (Figure 8), single distances sticking out of the dataset can be detected. Although the values have the appearance of statistical outliers, there was no justified explanation found from looking at the adjustment results, the images, etc. that would give reason for elimination of these values as outliers. The values must therefore be treated as real. Theoretically a couple of values may therefore exist in a measuring volume that deviate significantly from the given values of all ΔL. As the difference between these extreme values and some averaging value can be rather significant, it is important to report the LME for a measuring volume witch is the maximum absolute ΔL.

Internal precision of the adjustments indicated a coordinate precision of 0.010 mm and better for all cameras. Error propagation leads to a theoretical LME that can be estimated by equation (1) (Luhmann et al., 2006):

$$LME = 3 \cdot \sqrt{2} \cdot RMS_{XYZ} = \sqrt{18} \cdot RMS_{XYZ} \quad (1)$$

A RMS value of 0.01 mm yields a theoretical LMS of 0.042 mm, assuming a significance level of 99% (about 3 sigma). The measured results lie in the same range, proving the theoretical results.

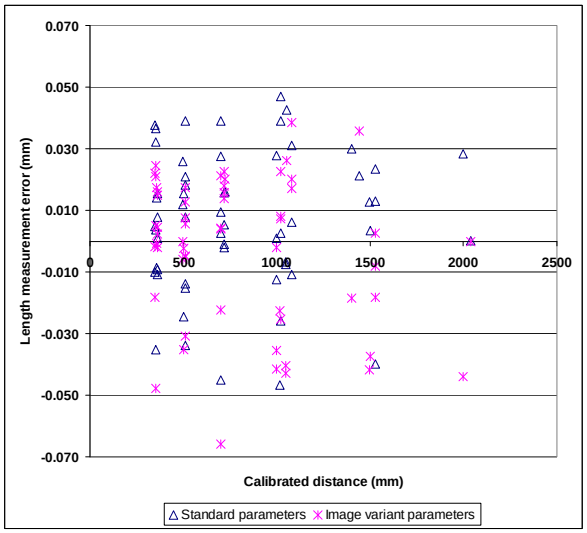

Figure 7. Length measurement errors ΔL of the Canon EOS 5D epoxy fixing resulting from standard calibrations and from image variant calibration.

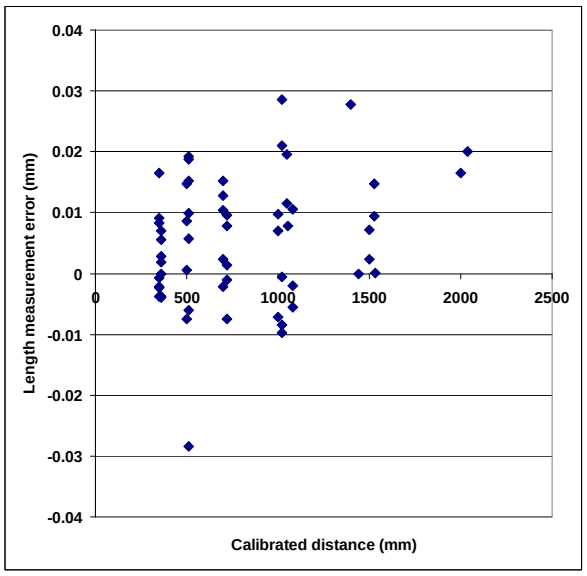

Figure 8. Length measurement error ΔL of the Alpa 12 WA calibrated with image variant interior orientation.

4. CONCLUSION

Calibration and accuracy evaluation of different camera setups on the test cube reveals not only different levels of accuracy for different camera models, but also reasons for geometric instabilities of digital cameras that are not designed for photogrammetry. Mounting a ringflash to the lens has the largest negative effect on accuracy in object space. This indicates that the ringflash should not be mounted to the lens and that the focusing tube of the lens is the geometrically weakest point in the processing chain. Mounting a ringflash next to the lens is therefore advisable. At the same time a fixation of the lens tube, as being done for the Canon EOS 5D in one setup, should fix the major cause of geometric instability. In case of the EOS 5D with fixation of the lens tube, the ringflash is mounted to the lens and the camera still yields the

best overall LME with a standard calibration. Fixation of the Canon lens does not affect any camera features like exposure measuring, open aperture metering or data retrieval for EXIF-files, besides focusing.

Parameterization of instable camera geometry by means of image variant interior orientation helps to uncover the potential accuracy of cameras. Further testing will be required to check how much of the accuracy potential may be unleashed by mechanical stabilization of cameras, or just by unloading the weight of the ringflash off the lens. Since most software products do not allow working with calibration results other than the standard set of parameters, parameterization should not be understood as a universal solution for fixing the geometric stability of cameras. In case of the EOS 5D as little as 10 g of epoxy for lens fixation had a greater effect in geometric stability than additional parameterization. For some cameras parameterization results in better maximum absolute LME values. It has to be tested if this effect is also visible for an extended parameterization set in non-optimal configurations, witch can be predicted in normal measuring environments using mechanical stabilized camera

REFERENCES

Haig, C., Heipke, C., Wiggenhagen, M., 2006. Lens inclination due to instable fixings detected and verified with VDI/VDE 2634 Part 1. *International Archives of Photogrammetry, Remote Sensing and Spatial Information Sciences,* Vol. 6, Part 5.

Hastedt, H., Luhmann, T., Tecklenburg, W., 2002. Image-variant interior orientation and sensor modelling of high-quality digital cameras. *International Archives of Photogrammetry, Remote Sensing and Spatial Information Sciences*, 34(5), pp. 27-32.

Luhmann, T., Hastedt, H., Tecklenburg, W., 2006. Modelling of chromatic aberration for high precision photogrammetry. *International Archives of Photogrammetry, Remote Sensing and Spatial Information Sciences,* Vol. 36(5), pp. 173-178.

Peipe, J. , Schneider, C.-T., 1995. High resolution still video camera for industrial photogrammetry. *Photogrammetric Record* 15 (85), pp. 135-139.

Rieke-Zapp, D., Nearing, M., 2005. Digital close range photogrammetry for generation of digital elevation models from soil surfaces. *Photogrammetric Record,* 20(109), pp. 69-87.

Shortis, M. R., Bellman, C. J., Robson, S, Johnston, G. J., Johnson, G. W., 2006. Stability of zoom and fixed lenses used with digital SLR cameras. *International Archives Photogrammetry and Remote Sensing,* 36(5), pp. 285-290.

Shortis, M. R., Ogleby, C. L., Robson, S., Karalis, E. M., Beyer, H. A., 2001. Calibration modelling and stability testing for the Kodak DC200 series digital still camera. *Proceedings, Videometrics and Optical Methods for 3D Shape Measurement,* SPIE Vol. 4309, pp 148-153.

AICON, 2007. AICON 3D Studio – Handbuch. Software manual on CD-ROM.

AXIOS, 2008. http://www.axios3d.de/downloads/handbuecher/AX.Ori.Con1.8%20Handbuch%20V1.pdf (accessed 1 May 2008).

Gruen, A., Maas, H.-G., Keller, A., 1995. Kodak DCS 200 – a camera for high accuracy measurements? *SPIE Proceedings Videometrics IV,* Vol. 2598.

Rieke-Zapp, D., Oldani, A., Peipe, J., 2005. Eine neue, hochauflösende Mittelformatkamera für die digitale Nahbereichsphotogrammetrie. *Publikationen der DGPF*, Band 14, Seyfried, E. (ed.), Berlin, pp. 263-270.

Maas, H.-G., 1999. Ein Ansatz zur Selbstkalibrierung von Kameras mit instabiler innerer Orientierung. *Publikationen der DGPF*, Band 7, Munich, pp. 47-53.

Tecklenburg, W., Luhmann, T., Hastedt, H., 2001. Camera modelling with image-variant parameters and finite elements. *Optical 3-D Measurement Techniques V*, Gruen, A., Kahmen, H. (Eds.), pp. 328-335.

VDI/VDE, 2002. VDI/VDE 2634 Part 1, Optical 3D measuring systems – imaging systems with point-by-point probing. Beuth Verlag, Berlin.